

# Molecular dynamics study of cage decay, near constant loss and crossover to cooperative ion hopping in lithium metasilicate

メタデータ	言語: eng 出版者: 公開日: 2017-10-03 キーワード (Ja): キーワード (En): 作成者: メールアドレス: 所属:
URL	<a href="http://hdl.handle.net/2297/1707">http://hdl.handle.net/2297/1707</a>

# Molecular dynamics study of cage decay, near constant loss, and crossover to cooperative ion hopping in lithium metasilicate

J. Habasaki

*Tokyo Institute of Technology, Nagatsuta 4259, Yokohama 226-8502, Japan*

K. L. Ngai

*Naval Research Laboratory, Washington, DC 20375-5320*

Y. Hiwatari

*Kanazawa University, Kakuma, Kanazawa 920-1192, Japan*

(Received 24 February 2002; published 26 August 2002)

Molecular dynamics (MD) simulations of lithium metasilicate ( $\text{Li}_2\text{SiO}_3$ ) in the glassy and supercooled liquid states have been performed to illustrate the decay with time of the cages that confine individual  $\text{Li}^+$  ions before they hop out to diffuse cooperatively with each other. The self-part of the van Hove function of  $\text{Li}^+$  ions,  $G_s(r,t)$ , is used as an indicator of the cage decay. At 700 K, in the early time regime  $t < t_{x1}$ , when the cage decays very slowly, the mean square displacement  $\langle r^2 \rangle$  of  $\text{Li}^+$  ions also increases very slowly with time approximately as  $t^{0.1}$  and has weak temperature dependence. Such  $\langle r^2 \rangle$  can be identified with the near constant loss (NCL) observed in the dielectric response of ionic conductors. At longer times, when the cage decays more rapidly as indicated by the increasing buildup of the intensity of  $G_s(r,t)$  at the distance between  $\text{Li}^+$  ion sites,  $\langle r^2 \rangle$  broadly crosses over from the NCL regime to another power law  $t^\beta$  with  $\beta \approx 0.64$  and eventually it becomes  $t^{1.0}$ , corresponding to long-range diffusion. Both  $t^\beta$  and  $t^{1.0}$  terms have strong temperature dependence and they are the analogs of the ac conductivity [ $\sigma(\omega) \propto \omega^{1-\beta}$ ] and dc conductivity of hopping ions. The MD results in conjunction with the coupling model support the following proposed interpretation for conductivity relaxation of ionic conductors: (1) the NCL originates from very slow initial decay of the cage with time caused by few independent hops of the ions because  $t_{x1} \ll \tau_o$ , where  $\tau_o$  is the independent hop relaxation time; (2) the broad crossover from the NCL to the cooperative ion hopping conductivity  $\sigma(\omega) \propto \omega^{1-\beta}$  occurs when the cage decays more rapidly starting at  $t_{x1}$ ; (3)  $\sigma(\omega) \propto \omega^{1-\beta}$  is fully established at a time  $t_{x2}$  comparable to  $\tau_o$  when the cage has decayed to such an extent that thereafter all ions participate in the slowed dynamics of cooperative jump motion; and (4) finally, at long times  $\sigma(\omega)$  becomes frequency independent, i.e., the dc conductivity. MD simulations show the non-Gaussian parameter peaks at approximately  $t_{x2}$  and the motion of the  $\text{Li}^+$  ions is dynamically heterogeneous. Roughly divided into two categories of slow (A) and fast (B) moving ions, their mean square displacements  $\langle r_A^2 \rangle$  and  $\langle r_B^2 \rangle$  are about the same for  $t < t_{x2}$ , but  $\langle r_B^2 \rangle$  of the fast ions increases much more rapidly for  $t > t_{x2}$ . The self-part of the van Hove function of  $\text{Li}^+$  reveals that first jumps for some  $\text{Li}^+$  ions, which are apparently independent free jumps, have taken place before  $t_{x2}$ . While after  $t_{x2}$  the angle between the first jump and the next is affected by the other ions, again indicating cooperative jump motion. The dynamic properties are analogous to those found in supercooled colloidal particle suspension by confocal microscopy.

DOI: 10.1103/PhysRevE.66.021205

PACS number(s): 61.20.-p, 63.50.+x

## I. BACKGROUND

The most commonly used experimental technique to probe the ions is electrical conductivity relaxation that measures the macroscopic dielectric response of a sample as a function of frequency. The conductance and capacitance of the sample are usually measured and from the results the complex dielectric susceptibility  $\epsilon^*(\omega)$  and complex conductivity  $\sigma^*(\omega)$  are obtained [1–10], or directly the complex electric modulus  $M^*(\omega)$  is obtained [11,12]. The frequency dependence of data in the complex conductivity representation usually is well described by using Jonscher's expression [7]

$$\sigma^*(\omega) \equiv \sigma'(\omega) + i\sigma''(\omega) = \sigma_0 [1 + (i\omega/\omega_p)^{n_J}], \quad (1)$$

where  $\sigma_0$  is the dc conductivity,  $\omega_p$  a characteristic relax-

ation frequency, and  $n_J$  a fractional exponent. On the other hand, the same data in the electric modulus representation are also well described by the one-sided Fourier transform,

$$M^*(\omega) = M' + iM'' = M_\infty \left[ 1 - \int_0^\infty dt \exp(-i\omega t) (-d\Phi/dt) \right] \quad (2)$$

of the Kohlrausch stretched exponential function [1–5,13]

$$\Phi(t) = \exp[-(t/\tau)^{1-n}]. \quad (3)$$

The  $\sigma'(\omega)$  obtained from Eqs. (2) and (3) is similar to the Jonscher's expression in having the dc conductivity at low frequencies and increases as a power law  $(\omega\tau)^n$  at high frequencies.

Traditionally, the study of the dynamic response of ionic conductors is focused on the motion of the ions that contribute to diffusion and conductivity. Whatever the preferred representation of the data and the empirical expression used to describe them,  $\sigma_0$  and  $\omega_p$  in Eq. (1) and  $\tau$  in Eqs. (2) and (3) are all thermally activated with about the same activation energy, indicating that they are originating from the migration of ions from one site to another after overcoming the energy barrier confining them in their potential wells by thermal activation.

However, there is another ubiquitous contribution to ac conductivity that until recently has received little attention. This contribution consists of a nearly frequency independent dielectric loss [hence referred to in the literature as the near constant loss (NCL) [4,6,14–21]],  $\varepsilon''(\omega) \approx A\omega^\alpha$ , where  $\alpha$  is nearly zero and  $A$  is a constant with weak temperature dependence that is approximately described by  $\exp(T/T_0)$ . The NCL corresponds to an almost linear frequency dependent term  $\sigma'(\omega) = \omega\varepsilon''(\omega) \approx A\omega^{1-\alpha}$  in the real part of the complex conductivity. At sufficiently low temperature or high frequencies, this near  $A\omega$  term dominates over the ion hopping ac conductivity term which has the fractional power law  $\omega^{n/2}$  from the Jonscher's expression or  $\omega^n$  from Eqs. (2) and (3). The properties of the NCL differ [19] in many respects from the ion hopping transport contribution and can be considered to have different physical origins. From the properties of the NCL, it was concluded that it comes from the ions [19]. The evidences include the observed approximately linear increase of the NCL with concentration of the mobile ions [16], and the existence of NCL in crystalline ionic conductors [19–21].

## II. VERY SLOW CAGE DECAY AS THE MECHANISM FOR THE NCL

In a recent paper [21] an analysis of the constant loss contribution to the ac conductivity, in the frequency range 10 Hz–1 MHz and finely spaced temperatures down to 8 K, was reported for two different Li ionic conductors, one crystalline ( $\text{Li}_{0.18}\text{La}_{0.61}\text{TiO}_3$ ) and the other glassy ( $61\text{SiO}_2 \cdot 35\text{Li}_2\text{O} \cdot 3\text{Al}_2\text{O}_3 \cdot 1\text{P}_2\text{O}_5$ ). At lower temperatures, a NCL corresponding to linear frequency dependent ac conductivity is the dominant contribution. As temperature is increased a crossover from the near constant loss to a fractional power law frequency dependence of the ac conductivity [Eq. (1) or Eqs. (2) and (3)] is observed. At any fixed frequency  $\omega$ , this crossover occurs at a temperature  $T$  determined approximately by the relation

$$\omega \approx \omega_\infty \exp(-E_m/kT). \quad (4)$$

Here  $\omega_\infty$  is an attempt frequency and  $E_m$  is the activation energy, which turns out to be significantly smaller than the dc conductivity activation energy, and it has been identified with the energy of the barrier preventing the  $\text{Li}^+$  ions to jump out from their potential wells. Later on, similar crossover from NCL to ion hopping ac conductivity was found [22] in the glass-forming molten salt  $0.4\text{Ca}(\text{NO}_3)_2 - 0.6\text{KNO}_3$  (CKN) from data [23,24] at temperatures above and below its glass transition temperature. Furthermore, it

was found [22] at all temperatures that the reciprocal of the independent relaxation time of the ions of the coupling model [25–30] for ionic conductivity relaxation [9,31–35] lies within the crossover region. The independent relaxation times  $\tau_o$  were calculated from the parameters  $n$  and  $\tau$  obtained to fit isothermal data of  $M^*(\omega)$  of CKN by Eqs. (2) and (3) and the relation [9,25–35] between  $\tau$  and  $\tau_o$ ,

$$\tau = [t_c^{-n} \tau_o]^{1/(1-n)} \quad (5)$$

with  $t_c = 1$  to 2 ps determined previously by high frequency measurements for ionic conductors including CKN [9,10,35–37]. Since  $\tau_o$  of the coupling model is the thermally activated relaxation time of an ion to overcome the barrier and hop out of its own well independent of the other ions, the good agreement between the experimentally determined crossover region and location of the independent relaxation frequency (i.e., the reciprocal of  $\tau_o$ ) is unsurprising after all. The good agreement supports the interpretation advanced [21,22] that the NCL is the loss due to very slow cage decay by few and infrequent hops of ions out of their cages, while the majority of the ions are still being caged. The NCL is terminated at sufficient long times  $t_{x1}$  when the fraction of ions that have independently jumped out of their cages is not small and the cage decay is no longer very slow. At still longer times, after a significant fraction of ions have made their independent jumps out of their wells, the ions can move longer distances but only in a cooperative manner due to their mutual interaction/correlation. Exemplified by ac conductivity, the cooperative ion dynamics give rise to the ion hopping contribution described by the Kohlrausch function in the electric modulus representation, Eqs. (2) and (3). Cooperative dynamics slows down further hops of the ions and explains that  $\tau$  in Eqs. (3) and (5) is much longer than  $\tau_o$ . Naturally, a measure of the time for a significant fraction of the ions to have independently jumped out of their cages is given by the thermally activated relaxation time  $\tau_o$ . Therefore the onset time  $t_{x2}$  of ion hopping ac conductivity described by Eqs. (2) and (3) is expected to be longer than  $\tau_o$ .

For a fixed cage with a potential that does not change with time, there is no NCL that extends over decades of time and increases in extent with decreasing temperature like that found in ionic conductors. In a harmonic well, the mean square displacement of the ion, given by Chandrasekhar [38], increases rapidly with time to a maximum value that is proportional to  $T$ . If the cage confining an ion in ionic conductors decays with time, then obviously a loss is observable while the ion still remains in the decaying cage. This loss can be observed as an increase of the mean square displacement  $\langle r^2 \rangle$  of the ions with time, in response to the decay of the cage. If the cage decay is a sufficiently slow function of time, the corresponding increase of  $\langle r^2 \rangle$  is correspondingly also slow. In general, the cage or potential well confining a mobile ion is determined by the matrix atoms and other mobile ions nearby, as evident from the form of typical potentials used in molecular dynamics simulations [39–49]. The cage is not permanent and it changes or decays because of at least

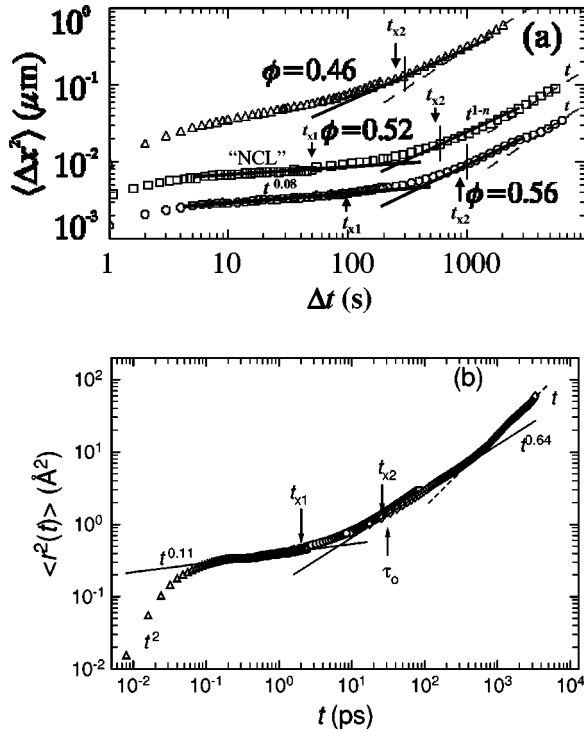


FIG. 1. (a) Mean square displacement (MSD) of colloidal particles in colloidal supercooled liquids with three different volume fractions as a function of delay time (redrawn from the data of Weeks and Weitz [58]). The time  $t_{x1}$  marks the end of the very slow rise of the MSD with logarithm of time approximately  $t^{0.08}$ . In the time regime  $t_{x1} < t < t_{x2}$ , the slope continue to increase. After  $t_{x2}$ , the MSD is well described by a fractional power law  $t^{1-n}$  until it finally assumes the  $t^{1.0}$  dependence at the longest times. (b) Mean square displacements of Li ions at 700 K.  $t_{x1}$  and  $t_{x2}$  are crossover times that separate out three time regimes as explained above and in the text.  $\tau_0$  is the independent free jump relaxation time of the Li ion calculated from Eq. (5) of the coupling model.

two reasons. First, the spatial relation of the mobile ion with the matrix atoms can change with time as suggested by the broadening of the first peak of the self-part of the van Hove function of the mobile ion,  $G_s(r, t)$ , with time as will be shown later. Second, some of the other ions nearby may have left their cages and the probability of them doing so increases with time. The second contribution to cage decay was established by study of the motion of concentrated colloidal particle suspension using confocal microscopy by Weeks and Weitz [50]. In this case, the cage is formed entirely by neighboring particles of the same kind as the caged particle. By defining particles as nearest neighbors if their separation is less than a cutoff distance set by the first minimum of the pair correlation function, Weeks and Weitz define a cage correlation function  $C_{\text{cage}}(\Delta t)$  by the fraction of particles with the same neighbors at time  $t$  and at  $t + \Delta t$ , after averaging over all  $t$ . Deduced from the confocal microscopy data,  $C_{\text{cage}}(\Delta t)$  shows decay with  $\Delta t$ . At short times,  $C_{\text{cage}}(\Delta t)$  decays very slowly, and concomitantly the mean square displacement of the particles  $\langle r^2(\Delta t) \rangle$  increases very slowly. In fact, from the data reported by Weeks and Weitz for volume fraction equal to 0.52 and 0.56, we observe that

$\langle r^2 \rangle$  increases approximately as  $c(\Delta t)^\alpha$  with  $\alpha \approx 0.08$  in the time regime of roughly between 7–50 s and 5–130 s, respectively [see Fig. 1(a) here], where  $C_{\text{cage}}(\Delta t)$  exhibits also very slow decay [see Fig. 2(b) of Ref. [50]]. Such a slow increase of  $\langle r^2 \rangle$  with time is equivalent to a NCL if the particle is charged and the quantity measured is dielectric loss due to conductivity relaxation. This result can be seen from the following relation between mean square displacement and complex conductivity:

$$\sigma^*(\omega) = -\omega^2 \frac{Nq^2}{6H_R kT} \int_0^\infty \langle r^2(t) \rangle e^{-i\omega t} dt, \quad (6)$$

where  $N$  is the density of mobile ions,  $q$  the ion charge,  $k$  the Boltzmann's constant,  $H_R$  the Haven ratio, and  $T$  the temperature [51]. For  $\langle r^2 \rangle \propto ct^\alpha$ , Eq. (6) gives  $\sigma'(\omega) \propto \omega^{1-\alpha}$ ,  $\sigma''(\omega) \propto \omega^{-\alpha}$ , and therefore a NCL, if  $\alpha$  is small.

The colloidal particles system studied by Weeks and Weitz [50] offers support of the proposed physical origin of the NCL as due to cage decay in the time regime where the decay is a very slowly varying function of time [21,22]. In this work, we demonstrate by molecular dynamics (MD) simulation that the same is true for the  $\text{Li}^+$  ions in lithium metasilicate glass. The existence of the NCL is shown by a very slow increase of  $\langle r^2 \rangle$  with time, and its origin identified with a very slow cage decay is inferred from the time dependence of the self-part of the van Hove function. The crossover times  $t_{x1}$  and  $t_{x2}$  are found and the proximity in order of magnitude of  $t_{x2}$  with  $\tau_0$  is verified. Other properties including time and temperature dependences of the non-Gaussian parameter, and the heterogeneous dynamics of the  $\text{Li}^+$  ions are shown to be similar to the colloidal supercooled liquids [50] and the Lennard-Jones liquid.

### III. RESULTS FROM MOLECULAR DYNAMICS SIMULATION

In previous works, we have examined the jump relaxation processes in lithium and mixed alkali metasilicate glasses by MD simulations [44–49]. In the present work, we have acquired additional MD data of lithium metasilicate ( $\text{Li}_2\text{SiO}_3$ ) glass at a low temperature for a different purpose. The objective is to show the existence of the NCL, its relation to the decay of the cage, and its gradual transition (or broad crossover) at longer times to ion hopping ac conductivity. MD simulations were performed in the same way as in previous studies [44–49]. Contained in the unit cell are 144 Li, 72 Si, and 216 O for  $\text{Li}_2\text{SiO}_3$ . The volume was fixed as that derived by NPT (constant pressure and temperature) ensemble simulation at atmospheric pressure. Pair potential functions of Gilbert-Ida-type [52] and  $r^{-6}$  terms were used. The parameters of the potentials used were previously derived on the basis of *ab initio* molecular orbital calculations [53], and their validity was checked in the liquid, glassy, and crystal states under constant pressure conditions. The system was equilibrated at 4000 K for more than 10 000 time steps, starting from a random configuration, and then the system was cooled to lower temperatures in order of 3000, 2000, 1673, 1473, 1200, 1000, 900, 800, 700, and 500 K. At each tem-



perature, the system was equilibrated adequately. The glass transition temperatures obtained by  $T$ - $V$  relation was approximately 830 K. The runs for  $\text{Li}_2\text{SiO}_3$  system at 700, 800, 1000, and 1200 K were analyzed.

For the purpose of this work, the statistics of the data was improved compared with that reported in the previous published works. MD runs, 1–4 ns (250 000–1 000 000 steps), were performed for  $\text{Li}_2\text{SiO}_3$  system at several temperatures. Using a sequence of particle positions during a run of  $T_1$  period, we prepared  $N$  arrays of data sequence with slightly shifted initial time  $t_0$  values and the data for  $N$  arrays were averaged. Then the time window  $\delta t$  is a time range covered by chosen  $t_o$  values. In a rapidly decaying system such as a normal liquid, the time window of several tens picoseconds is long enough to obtain the macroscopic values. However, in the glassy state some properties depend on the time scale of observation, which is determined by the value of  $\delta t$ . A time window of 80 ps at higher temperatures, 400 ps at lower temperatures, and  $N$  ranging from 200 to 400 were used in the present work. In this work, we focus our attention on the motion of the  $\text{Li}^+$  ions. Information on the relaxation dynamics of the matrix atoms, Si and O, in the liquid and glassy states can be found in Refs. [46,48]. Comparison between the  $\text{Li}^+$  ion diffusion data from simulation and experimental conductivity relaxation data in  $\text{Li}^+$  metasilicate glass have been made but will not be reported here.

### A. Mean square displacement

Mean square displacement (MSD) of Li ions  $\langle r^2 \rangle$  at 700 K is shown in Fig. 1(b) from 0.01 ps to a few thousand picoseconds. At very short times we see the ballistic motion that has  $\langle r^2 \rangle \propto t^2$  and then a combination of vibrational and relaxation contribution at longer times as discussed in the previous works [48,49]. Vibrational contribution to the MSD becomes constant after about 1 ps. The  $\text{Li}^+$  MSD of present interest can be divided into four time regimes.

(1) At an early time regime between approximately 0.3 and 2 ps, where the MSD increases very slowly with time approximately as  $t^\alpha$  with  $\alpha \approx 0.1$ , the MSD can be identified with the NCL. The description here of the MSD by a power law  $t^\alpha$  with  $\alpha \approx 0.1$  follows the tradition of dielectric measurement of glassy ionic conductors in modeling the NCL by also a power law  $\epsilon''(\omega) \approx A \omega^\alpha$ , where  $\alpha$  is a small positive number. Actually from our data we can only say that the increase of MSD is very slow in the regime  $0.3 \leq t < 2$  ps, but the time dependence may be fit by other functions than the power law. In later sections we give physical arguments to justify the very slow increase of the MSD, and near the end of Sec. III B we mention another function that fits it as well.

(2) In the intermediate time regime of about  $2 < t < 20$  ps, the MSD rises more rapidly than  $t^\alpha$  of regime 1. The crossover from regime 1 to regime 2 defines a crossover time called  $t_{x1}$ , which is 2 ps at 700 K. Thus regime 1 is defined by  $0.3 \text{ ps} < t < t_{x1}$ . The value of  $t_{x1}$  is determined operationally to be the time beyond which the data deviates by more than 10% from the fit using the power law  $t^\alpha$  with  $\alpha \approx 0.1$  shown in Fig. 1(b).

(3) After 26 ps and up to about 400 ps, the MSD has a time dependence well described by  $t^\beta$  with  $\beta \approx 0.64$ . This is the time regime 3, which corresponds to the  $\omega^{1-\beta}$  power law ac conductivity for cooperative ion hopping predicted by the KWW expression [Eqs. (2) and (3) with  $\beta$  identified with  $1-n$ ]. The time when the time regime 3 starts defines  $t_{x2}$ , which is equal to 26 ps at 700 K. Thus regime 2 is defined by  $t_{x1} < t < t_{x2}$ . The value of  $t_{x2}$  is determined operationally to be the time before (after) which the data deviates by more (less) than 10% from the fit using the power law  $t^\beta$  with  $\beta \approx 0.64$  shown in Fig. 1(b).

(4) At time longer than about 600 ps, the MSD assumes the linear  $t$  dependence. At the starting time of this time regime, the root MSD  $\sqrt{\langle r^2 \rangle}$  is about 3 Å, the average distance between neighboring Li sites. In this time regime, the steady state of the cooperative ion hopping has been established and the MSD corresponds to the frequency independent dc conductivity. The onset time of this regime  $t_D$  (about 600 ps at 700 K) is not exactly the same as  $\tau$  of Eq. (3) but equal in order of magnitude. Thus approximately, regime 3 is defined by  $t_{x2} < t < \tau$  and regime 4 correspond to  $t > \tau$ .

It is interesting to point out that same properties are found for colloidal supercooled liquid with volume fraction  $\phi$  equal to 0.52 and 0.56. The time evolution of the mean square displacement of the colloidal particles  $\langle r^2(\Delta t) \rangle$  reported by Weeks and Weitz [50] [Fig. 1(a)] can be divided into four regimes, demarcated by  $t_{x1}$ ,  $t_{x2}$ , and  $\tau$ , in exactly the same manner as for the MSD of the Li ions. Figures 1(a) and 1(b) show these four regimes and the locations of the two crossover times  $t_{x1}$  and  $t_{x2}$ . The similarity between the Li ion dynamics in Li metasilicate glass and colloidal supercooled liquids goes further than their MSD, as we shall see in Secs. III C and III D to follow. The similarity in the existence of a very slow increase of the MSD in the short time regime  $t < t_{x1}$  in both cases suggests that the plateaus in Fig. 1(a) of colloidal supercooled liquids, for  $\phi$  equal to 0.52 and 0.56, can be identified with the NCL in ionic conductors. Furthermore, the global similarity of Figs. 1(a) and 1(b) indicates the possibility that the same physics governs both colloidal supercooled liquids and ionic conductors.

### B. van Hove functions

The self-part of the van Hove function for the Li ion is defined by

$$G_s(r, t) = (1/N) \sum_{i=1}^N \langle \delta[r_i(t) - r_i(0) - r] \rangle, \quad (7)$$

where  $r$  is the distance traveled by the Li ion in a time  $t$ . The number of ions remaining in the original sites can be calculated from

$$N(t) = \int_0^{r_c} 4\pi r^2 G_s(r, t) dr, \quad (8)$$

where  $r_c$  is chosen to be 1.7 Å. The value is slightly larger than half of the distance between the Li ions,  $g_{\text{Li-Li}}^{\text{max}}(r)$ , given in the previous study [43], but the difference is understand-

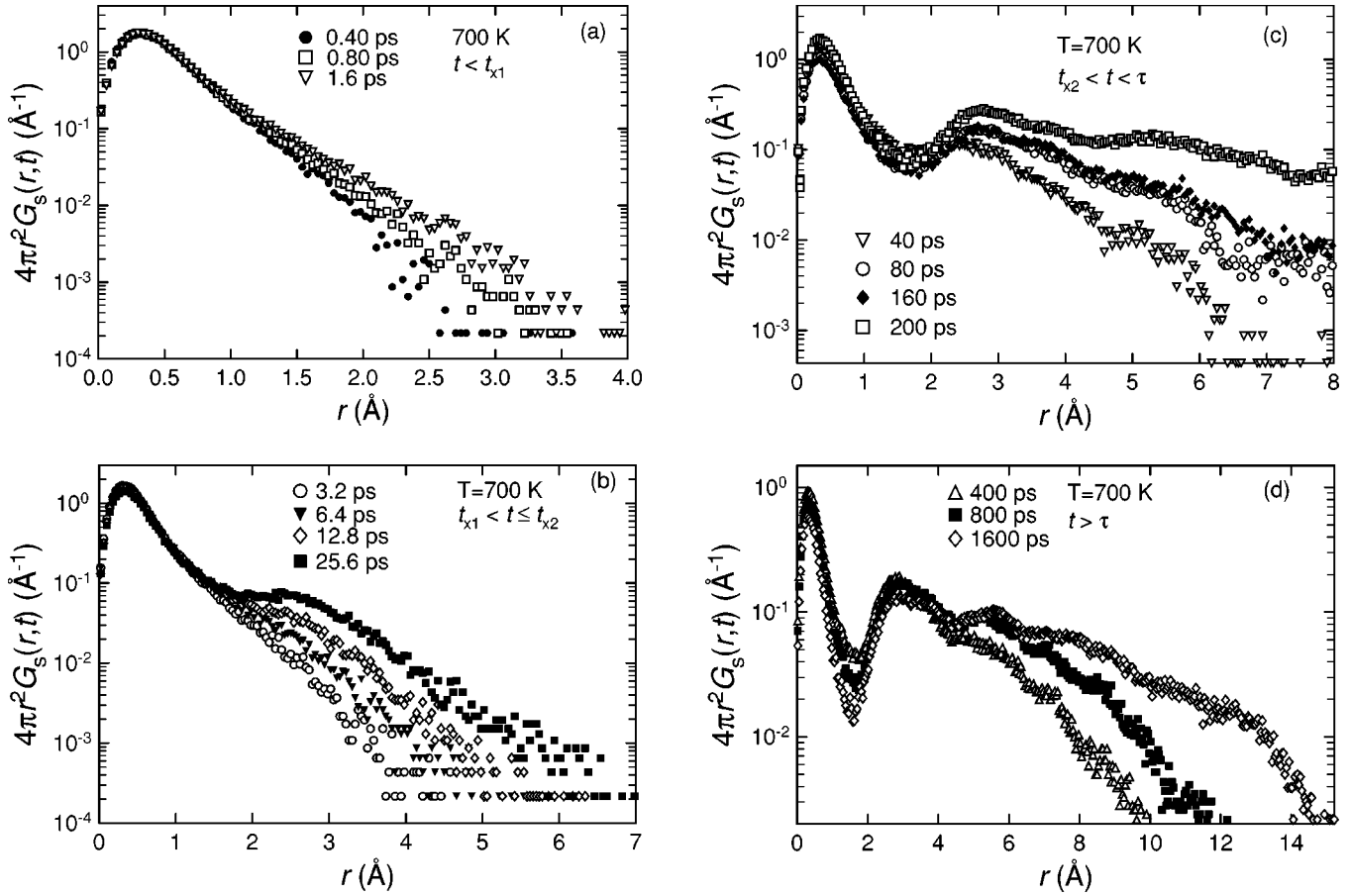


FIG. 2.  $4\pi r^2 G_s(r,t)$  as a function of  $r$  at different times.  $G_s(r,t)$  is the self-part of the van Hove function for the Li ion. (a) 0.40, 0.8, and 1.6 ps ( $t < t_{x1}$ ). (b) 3.2, 6.4, 12.8, and 25.6 ps ( $t_{x1} < t \leq t_{x2}$ ). (c) 40, 80, 160, and 200 ps ( $t_{x2} < t < \tau$ ),  $\tau \approx 229$  ps is calculated (see text). (d) 400, 800, and 1600 ps.

able because  $g_{\text{Li-Li}}(r)$  and  $G_s(r,t)$  are not the same quantity. Figures 2(a)–(d) show the evolution of  $4\pi r^2 G_s(r,t)$  as a function of  $r$  with time. Again we separate the evolution with time into several time regimes.

(i) The times in Fig. 2(a) from 0.4 to 1.6 ps are within the time regime 1 in which the MSD increases very slowly like  $t^\alpha$  with  $\alpha \approx 0.1$  and corresponds to the NCL in dielectric response of the glassy ionic conductor. There is only a slight increase of  $4\pi r^2 G_s(r,t)$  at near 3 Å with a concomitant small decrease in the area of the first peak. Using either one of these two quantities as indicator of the extent of the decay of the cage, we are led to conclude that the cage decay is indeed very slow. The broadening of the first peak of  $G_s(r,t)$  is also observed in this time region. Prejump motion and the changes in spatial relation of the mobile ion with the matrix atoms with time can be considered as origins of such broadening. Both are related to the jump motion of the  $\text{Li}^+$  ions and changes of the cage in a broader sense. Contribution of this broadening of the first peak of  $G_s(r,t)$  to MSD is not negligible, although our attention is focused on the area under the first peak of  $G_s(r,t)$  to gauge the decay of the cage in this work.

(ii) The times in Fig. 2(b) from 3.2 to 25.6 ps are nearly coincident with the time regime 2 in which the MSD increases more rapidly than in regime 1, but has not yet as-

sumed the constant fractional power law  $t^{1-n}$  with  $(1-n) \approx 0.7$ . A shoulder located at about 3 Å appears and grows in intensity with time indicating a more rapid cage decay than in time regime 1.

(iii) The times in Fig. 2(c) from 40 to 160 ps are within the time regime 3 in which the MSD has attained the power law dependence  $t^{1-n}$  with  $(1-n) \equiv \beta \approx 0.64$ . A second peak at about 3 Å is fully developed and a broad tail extended to longer distances appears, and both grow in intensity. The development of the second peak indicates that the number of ions that have left their original sites becomes significant. The cages have decayed to such an extent that most of ions are no longer caged and they participate in cooperative motion with each other. From Eq. (6), the power law dependence  $t^{1-n}$  of the MSD correspond to  $\sigma'(\omega) \propto \omega^n$ , which also follows from the electric modulus [Eq. (2)] after substitution of the electric field decay function therein by the Kohlrausch function [Eq. (3)]. The signature of cooperative ion hopping motion in time regime 3 also can be gleaned from the time dependence of the self-part of the Li ion density correlation function defined by

$$F_s(k,t) = \left\langle \frac{\sum_{j=1}^N \exp\{i\vec{k} \cdot (\vec{r}_j(t) - \vec{r}_j(0))\}}{N} \right\rangle \quad (9)$$

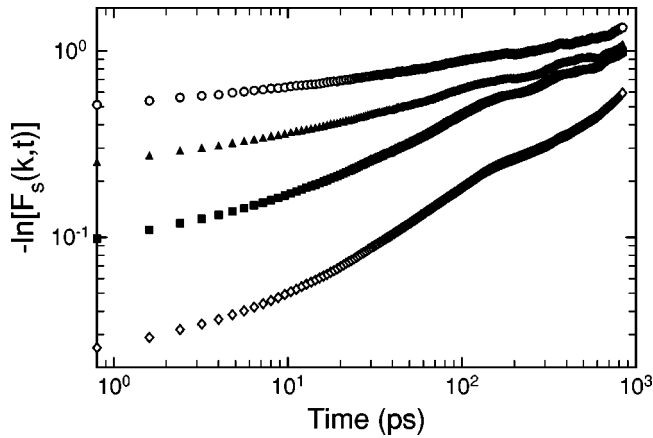


FIG. 3.  $\text{Log}\{-\ln[F_s(k,t)]\}$  vs  $\text{log } t$  plot for Li ions at 700 K. The curves from top to bottom correspond to  $k=2\pi/2.0$ ,  $2\pi/3.0$ ,  $2\pi/5.0$ , and  $2\pi/10.0 \text{ \AA}^{-1}$ , respectively.

In Fig. 3 we show plots of  $\text{log}\{-\ln[F_s(k,t)]\}$  against  $\text{log } t$  at 700 K for  $k=2\pi/2.0$ ,  $2\pi/3.0$ ,  $2\pi/5.0$ , and  $2\pi/10.0 \text{ \AA}^{-1}$ . Curves with small wave numbers in Fig. 3 have straight portions that starts at about 20 ps. Since the Kohlrausch stretched exponential form of Eq. (3) corresponds to the straight line in such a plot, therefore  $F_s(k,t)$  is a stretched exponential function of time at times longer than about 20 ps at 700 K. The slope of the straight portion of the curve is the stretch exponent  $(1-n)$ . It is to be noted that the stretch exponent is  $k$  dependent. For  $k=2\pi/10 \text{ \AA}^{-1}$ , the stretch exponent of  $F_s(k,t)$  from the slope for  $t>20$  ps is not too different from the exponent  $(1-n)\approx 0.64$  in the  $t^{1-n}$  dependence of the MSD in time regime 3. On the other hand, for  $k=2\pi/3.0 \text{ \AA}^{-1}$ , the stretched exponent of  $F_s(k,t)$  is noticeably smaller than that of the MSD. This difference as well as the dependence of  $(1-n)$  on  $k$  may originate from the stronger effect of ion-ion interaction in slowing down the dynamics at shorter distances (larger  $k$ ). An analogy of these findings is the difference between the ion dynamics probed by nuclear magnetic resonance and dc conductivity [54,55], which had been explained with the same reason. In any case, the stretched exponential time dependences of  $F_s(k,t)$  for several values of  $k$  are further indications of the onset of cooperative ion hopping motion at about 20 ps. The value of the onset time seems to become shorter for larger wave numbers and the change in the slope becomes less clear. Such plots of  $F_s(k,t)$  were used to also determine the onset of cooperative ion hopping at other temperatures.

(iv) At long times of 400, 800, and 1600 ps shown in Fig. 2(d), the second peak at  $\sim 3 \text{ \AA}$  has been fully developed and higher-order peaks become evident. In this time regime,  $\sqrt{\langle r^2 \rangle}$  starts at about 3  $\text{\AA}$  and the MSD of the Li ions has attained the  $t^{1.0}$  dependence shown in Fig. 1(b).

The starting point of stretched exponential decay at 1200 and 1000 K (both not shown) was found to be approximately equal to 1 and 2 ps, respectively. The change of van Hove function at 1200 K with time in the time regime of 0.2–2.2 ps is similar to that observed at longer times between 2 and 20 ps, i.e., regime 2,  $t_{x1} < t < t_{x2}$  at 700 K [see Fig. 4(b)]. The similarity shows that the times  $t_{x1}$  and  $t_{x2}$  are temperature

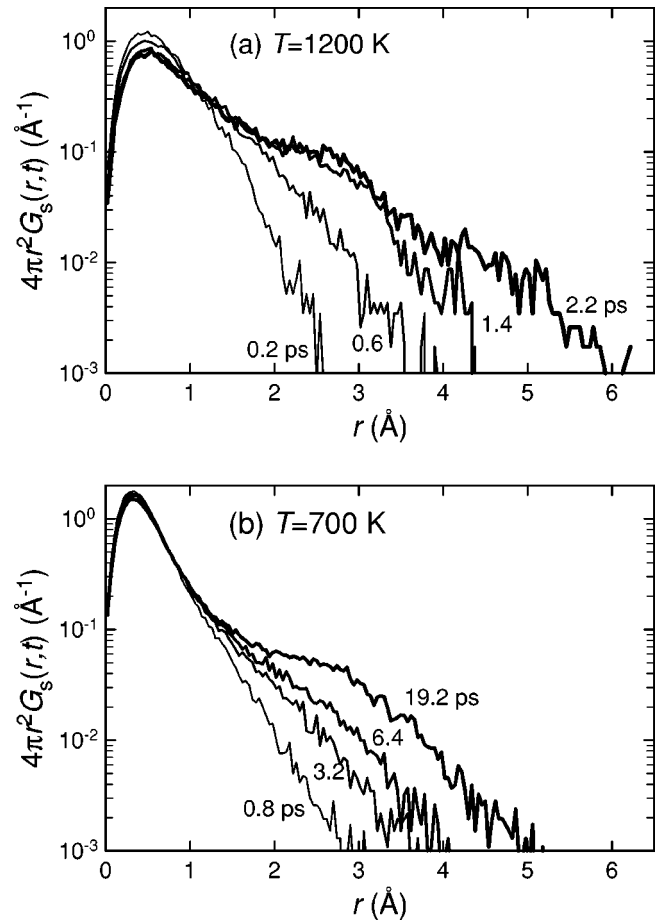


FIG. 4. Self-part of the van Hove functions of Li ions (a) at 1200 K and several times in the regime 0.2–2.2 ps and (b) at 700 K at several times in the regime 0.8–19.2 ps. The thicker curves are for the later times.

dependent, a feature that reappears in other quantities to be discussed below and found from conductivity relaxation data of CKN [22].

### C. Cage decay

In the early time regime between approximately 0.3 and 2 ps, the MSD increases very slowly with  $t$  like  $t^\alpha$  with  $\alpha \approx 0.1$  and has been identified with the NCL [21,22]. For ions confined in permanent harmonic and even anharmonic potential wells or cages, MSD does not have such a slow increase with time over an extended period of time as shown in Figs. 1(a) and 1(b), and certainly cannot explain the NCL observed experimentally over many decades of frequencies at lower temperatures in glassy and crystalline ionic conductors. However, the cages are not permanent. There is small but nonzero probability of the Li ions independently jumping out of their original sites by thermal activation even at short times. These independent jumps give rise to slow decay of the cages for some other ions that remained caged. The slow decay of the cage, the independent jumps, and the concomitant slow increase of the MSD are synergistic properties. If a cage correlation function can be defined and obtained from molecular dynamics simulation, like that done by Weeks and

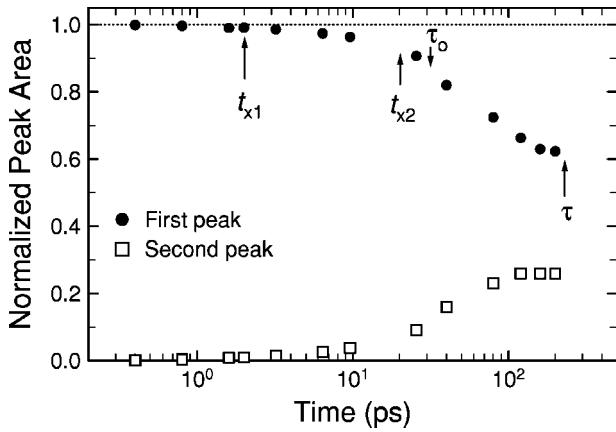


FIG. 5. Normalized areas of the first peak  $A_1(t)$  and the second peak  $A_2(t)$  of the self-part of the Li ion van Hove functions at 700 K at different times. The positions of  $t_{x1}$ ,  $t_{x2}$ ,  $\tau_o$ , and  $\tau$  are indicated by the vertical arrows.

Weitz [50] for colloidal particles from confocal microscopy experiment, the origin of NCL would come naturally from the slow decay of the cages. The loss can be related to the imaginary part of the Fourier transform of the cage decay correlation function. In this work, we obtain the time dependent decrease of the normalized area  $A_1(t)$  of the first peak of the self-part of the Li ion van Hove function at 700 K, and use it as a substitute to gauge the cage decay. Figure 5 shows the time dependence of  $A_1$  up to about 20 ps before the cooperative ion hopping time regime 3 where MSD has time dependence well described by  $t^\beta$  with  $\beta \approx 0.64$ . The decrease of  $A_1$  is very slow in time regime 1 between 0.3 and 2 ps, where the MSD increases very slowly with  $t$  as  $t^\alpha$  with  $\alpha \approx 0.1$ . Thus from the time dependence of  $A_1(t)$  in this time regime, the very slow cage decay is the origin of the NCL,  $\varepsilon''(\omega) \propto \omega^\alpha$  with  $\alpha \approx 0.1$ .

We have already mentioned that for the colloidal particles, the cage correlation function defined by Weeks and Weitz decays very slowly for times shorter than about 100 ps at volume fraction equal to 0.52 and 0.56 [see Fig. 2(b) of Ref. [50]]. Again this cage decay and the very gradual increase of  $\langle r^2(\Delta t) \rangle$  approximately as  $c(\Delta t)^\alpha$  with  $\alpha \approx 0.08$  are synergistic properties, analogous to the Li ions in the Li metasilicate glass. The ultimate origin of these two synergistic properties and the NCL in colloidal supercooled liquids as well as in the Li metasilicate is the occurrence of independent thermal activated jumps of a small percentage of Li ions from their cages in an extend period of  $\ln t$ . The independent jump relaxation is an important part of the coupling model [25–34]. Its relaxation time  $\tau_o$  is thermally activated with activation energy  $E_a$ , which is the same as the microscopic energy barrier and prefactor equal to the reciprocal of a vibrational attempt frequency. It has been determined or deduced in several ways from experiments [30–37, 54–56], and is related to the longer cooperative hopping relaxation time  $\tau$  by Eq. (5) [9, 30–40], where  $t_c$  is about 1 ps for alkali oxide glasses. At 700 K,  $\tau \approx 229$  ps from the previously determined stretched exponential relaxation time [43] of  $F_s(k, t)$  for  $k = 2\pi/3 \text{ \AA}^{-1}$ . Such  $k$  is chosen because it corresponds to

$\sqrt{\langle r^2 \rangle} \approx 3 \text{ \AA}$ , the distance between Li sites. This together with  $(1-n) \equiv \beta = 0.64$ ,  $t_c = 1$  ps, and Eq. (5) enables us to calculate  $\tau_o$  and the result is 32 ps, which is an order of magnitude longer than  $t_{x1}$  but is nearly the same as  $t_{x2}$ . This comparison between  $\tau_o$  and  $t_{x1}$  (i.e.,  $\tau_o$  significantly longer than  $t_{x1}$ ) explains the small probability of independent jump of the ions out of their cages during the time regime 1,  $t < t_{x1}$ , and the very slow decay of the cage indicated by either the MSD or  $A_1$  from the van Hove function (Fig. 5). However, in time regime 2,  $t_{x1} < t < t_{x2}$ , there is higher probability for independent jumps and the dependence  $\langle r^2 \rangle \propto t^\alpha$  with  $\alpha \approx 0.1$ , which defines the NCL, no longer holds. On increasing time towards  $t_{x2}$ , more ions independently hops out because  $t_{x2}$  is about the same as  $\tau_o$ . Therefore the cage decays more rapidly in regime 2 than in regime 1, a property corroborated by the time dependence of  $A_1$  in Fig. 5 and the MSD in Fig. 1(b). Near the end of the time regime 2 many more ions are hopping out and some such independent hops may be prohibited due to interaction and correlation between the ions. Some degree of cooperativity develops and increases with increasing time in regime 2. Since  $t$  is longer than  $\tau_o$  in most of regime 3,  $t_{x2} < t < \tau$ , all of the mobile Li ions have high probability of executing the independent jump, i.e.,  $\exp(-t/\tau_o)$  becomes small. However, simultaneous independent jumps of such a large number of ions are not possible because of the interaction and correlation between the ions. The only option left for the ions is to participate in the slowed down cooperative or correlated transport process that is dynamically heterogeneous. The stretched exponential correlation function for  $F_s(k, t)$  in regime 3 shown in Fig. 3 describes the fully cooperative hopping with participation of all mobile ions. Thus  $t_{x2}$  marks the change to the fully cooperative or correlated jump process modified by jump angles [42–48] of the successive jumps. Again this description is corroborated by even more rapid decrease of  $A_1$  in regime 3 than in regime 2, as can be seen by inspection of Fig. 5, and the steeper rise of the MSD with the power law dependence of  $t^\beta$  with  $\beta \approx 0.64$  in regime 3 [see Fig. 1(b)]. The same is true for the colloidal supercooled liquid. In the time regime  $t_{x1} < t < t_{x2}$  in Fig. 1(a), the cage correlation function [see Fig. 2(b) of Ref. [50]] decays faster than when  $t < t_{x1}$ . The decay is even faster when  $t > t_{x2}$ .

In our present as well as in previous simulations, the localized independent jumps occur at intervals longer than the relaxation time obtained from the jump rate, indicating that there are particles having high probability of jumping back into their original sites even in the region  $t < t_{x2}$  and only a net change of the number of the particles is reflected in the peak area of the van Hove functions. Therefore in time regime 1 and part of regime 2, where the  $\text{Li}^+$  ions make only independent or uncorrelated jumps, the contribution to MSD by ions that have successfully made the uncorrelated jumps,  $\langle r^2 \rangle_u$ , is proportional to  $t$  and less than  $d^2(t/\tau_o)$ , where  $d$  is the localized independent jump distance of the  $\text{Li}^+$  ion. The result follows from the fact that the jumps are uncorrelated and their number is proportional to time. Now the MSD is the sum of the contributions from vibration, relaxation, and the independent jumps. The contribution to the MSD from



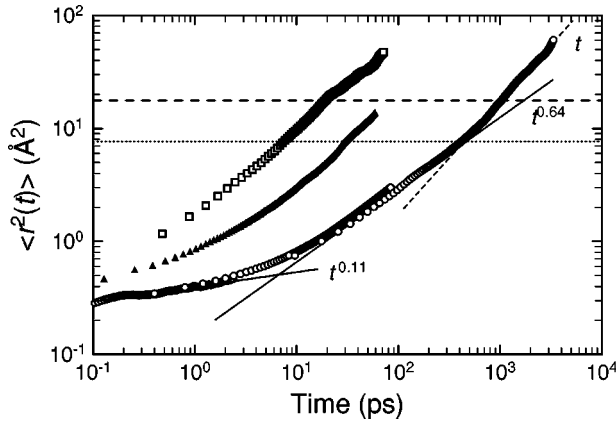


FIG. 6. Mean square displacements of Li ions at several temperatures: (○) 700 K, (▲) 1000 K, and (□) 1200 K, respectively. The dashed and dotted lines correspond, respectively, to the square of the distance of the first minimum ( $4.2 \text{ \AA}$ )<sup>2</sup>, and the square of the distance of the first maximum ( $2.77 \text{ \AA}$ )<sup>2</sup> of  $g(r)$  of Li-Li ions at 700 K.

Li<sup>+</sup> ion vibration,  $\langle r^2 \rangle_{\text{vib}}$ , initially increases with time and then turns over to the constant value  $kT/m\omega^2$ , where  $m$  is the mass and  $\omega$  the frequency, if the vibration is harmonic. Hence we may expect the sum  $\langle r^2 \rangle_{\text{vib}} + Ct$ , where  $C$  is a constant, gives not too bad a description of the time dependence of the MSD in regimes 1 and 2 when the contribution of relaxation ends. In these regions, the sum in fact is a good approximation to the data at 700 K. This result can be considered as another support for the slow increase in number of successful independent jumps as the origin of the NCL. Furthermore, in the NCL regime 1 at 700 K,  $\langle r^2 \rangle_u$  rises to no more than about 40% of  $\langle r^2 \rangle_{\text{vib}}$ . Hence the temperature dependence of the MSD is principally determined by  $\langle r^2 \rangle_{\text{vib}}$  but enhanced by the presence of the  $\langle r^2 \rangle_u$  term. Therefore, the temperature dependence of the MSD or the NCL in regime 1 is weak, and this may be used to rationalize the observed weak temperature dependence of the NCL in glassy ionic conductors [19].

Since  $\tau$  is thermally activated, at even lower temperatures than 700 K,  $\tau$  as well as  $\tau_o$  becomes much longer. At any time, the probability of independent ion jumps is further diminished. Consequently, the cage decay is even slower and  $t_{x1}$  and  $t_{x2}$  are extended to longer times. Therefore  $t_{x1}$  and  $t_{x2}$  are temperature dependent and we can expect that their temperature dependences are similar to that of  $\tau_o$ . On the other hand, at temperatures sufficiently higher than 700 K when  $\tau$  is not long compared with  $t_c$ ,  $\tau_o$  becomes short and  $t_{x1}$  and  $t_{x2}$  are moved to shorter times. Figure 6 shows the MSDs of Li ions at 1000 K and 1200 K in the supercooled liquid state. In exactly the same manner as done before for the data at 700 K,  $\tau$  is estimated to be 20 and 8 ps,  $(1-n) \equiv \beta = 0.70$ , and  $\tau_o$  calculated to be approximately 8 and 4 ps for  $T = 1000$  and 1200 K, respectively. The very short  $\tau_o$  of about 4 ps at 1200 K explains the earlier onset of the regime 3 at  $t_{x2}$ , which is estimated to be between 1 and 2 ps. The regime 2 is shifted to times shorter than 1 ps and regime 1 has disappeared into the vibrational contribution zone and no NCL can be observed.

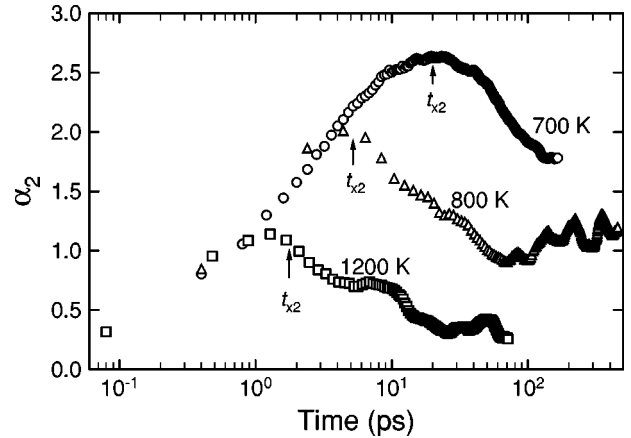


FIG. 7. The non-Gaussian parameter  $\alpha_2(t)$  of the Li<sup>+</sup> ions in Li<sup>+</sup> metasilicate calculated from their displacement distribution function of time at 700, 800, and 1200 K. At higher temperatures, the maximum of  $\alpha_2(t)$  of Li<sup>+</sup> ions moves to shorter times. At all temperatures, the maximum is located near  $t_{x2}$ .

#### D. The non-Gaussian parameter

The non-Gaussian parameter [57]

$$\alpha_2(t) = (3/5) \langle r^4(t) \rangle / \langle r^2(t) \rangle^2 - 1 \quad (10)$$

characterizes the deviation of  $G_s(r,t)$  from the Gaussian form. We have evaluated  $\alpha_2(t)$  of the Li<sup>+</sup> ions from their displacement distribution function of time at 700, 800 and 1200 K. The result plotted in Fig. 7 as a function of time shows that  $\alpha_2(t)$  starts out from small values at short times, increases throughout regimes 1 and 2, and attains maximum value near  $t_{x2} \approx 20$  ps and  $\tau_o \approx 32$  ps. At higher temperatures, the maximum of  $\alpha_2(t)$  of Li<sup>+</sup> moves to shorter times and it is also located near  $t_{x2}$  and  $\tau_o$  (Fig. 7). The occurrence of the maximum of  $\alpha_2(t)$  at a time near  $t_{x2}$  is found also in the colloidal supercooled liquids [58]. By inspection of Fig. 1(b) of Ref. [58], we locate the positions of the  $\alpha_2(t)$  peaks at 300, 500, and 1000 s for volume fractions of 0.46, 0.52, and 0.56, respectively. These peak positions are in remarkable agreement with  $t_{x2}$ . The values of  $t_{x2}$  from Fig. 1(a) are 235, 540, and 900 for volume fractions of 0.46, 0.52, and 0.56, respectively. Thus like colloidal supercooled liquids,  $\alpha_2(t)$  of Li<sup>+</sup> ions in metasilicate peaks near  $t_{x2}$ . Similar time-and-temperature dependences of  $\alpha_2(t)$  were found in molecular dynamics simulation of a supercooled Lennard-Jones liquid [59]. These similarities indicate once more that the same physics governs the dynamics of Li<sup>+</sup> ions in glasses as well as in colloidal supercooled liquid and in Lennard-Jones liquid. If this is indeed the case, then theory of fast relaxation that is applicable to the supercooled liquids but *not* to ions in glasses may not be the ultimate explanation that we are looking for.

#### E. Dynamic heterogeneities

The motion of the Li ions is dynamically heterogeneous, similar to that found in colloidal and Lennard-Jones supercooled liquids [58,59]. To illustrate this property for the Li<sup>+</sup>

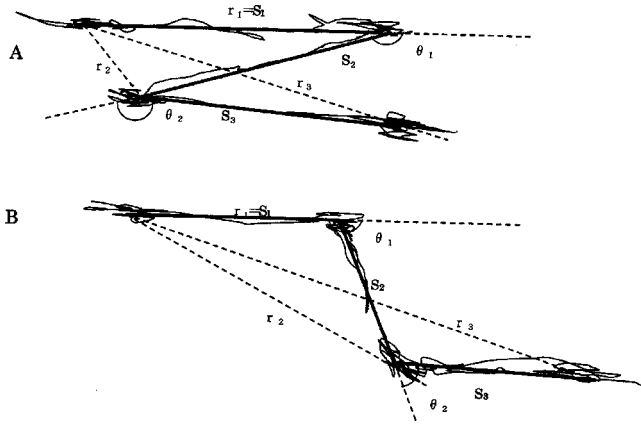


FIG. 8. Schematic description of jump motions for type-A  $\text{Li}^+$  ions (with large back correlation probability) and type-B  $\text{Li}^+$  ions (with large forward correlation probability). For both types of  $\text{Li}^+$  ions the displacement of the first jump  $r_1$  is the same (i.e., the typical jump distance  $s_1$ ), while the displacements after the first jump depend on the type of the  $\text{Li}^+$  ions due to consideration of the angles between consecutive jumps  $\theta$ . The situation is unchanged, even if we start from different initial time.

ions, we divided the ions into two groups. The particles showing a squared displacement less than the square of the distance equal to the first minimum of the Li-Li static structure factor  $g(r)$  is defined as type A. Namely, the ion is located within neighboring sites during a given time  $t^*$ . Particles showing a squared displacement greater than the square of the distance equal to the first minimum of  $g(r)$  are defined as type B, which can contribute to the long time dynamics. In the present work, type-A and type-B particles are distinguished by MSD using time window  $\delta t$  of 80 ps (100 points of initial  $t$ ) during  $t^*$  of 920 ps. The MSD of all Li ions shown in Fig. 1(b) is the weighted average of MSDs for type-A and type-B particles, i.e.,

$$\langle r^2(t) \rangle = (N_A \langle r_A^2 \rangle + N_B \langle r_B^2 \rangle) / N, \quad (11)$$

where  $\langle r_A^2 \rangle$  and  $N_A$  are the MSD and number of type-A ions, respectively. Similar definitions apply to the quantities for the type-B ions.

Initial parts of jump trajectory of the type-A and type-B particles at 700 K were schematically shown in Fig. 8. The MSD of type-A and type-B ions are plotted as a function of time in Fig. 9. In the first jump, the jump distance is the same for both types A and B. The MSDs of the ions of both types are almost the same until  $t_{x2}$  is reached. This is just as expected from an explanation afforded by Fig. 8. Both type-A particles (with high probability of backward correlated jumps) and type-B particles (with high probability of forward correlated jumps) behave as if they jumped freely or independently before  $t_{x2}$ . Note that even if we start the observation from any jump, the first jump looks like a free jump, since the displacement is not modified by jump angles. This does not mean that the every jump is without any influence of the other ions. Therefore, the free jump is apparent and every jump is under influence of the other ions.

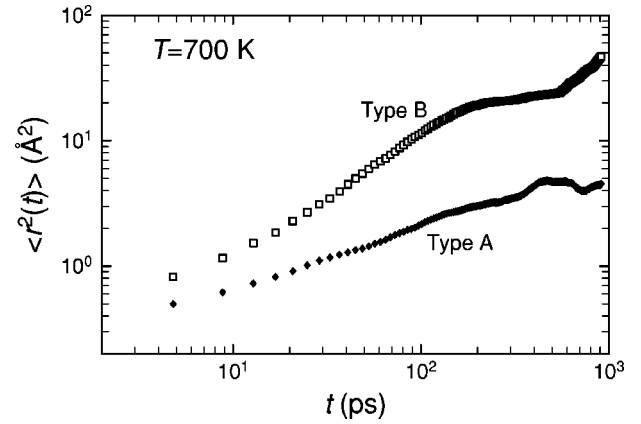


FIG. 9. The MSDs of type-A (filled diamonds) and type-B (open squares)  $\text{Li}^+$  ions at 700 K. They bifurcate significantly at times near the broad maximum of non-Gaussian parameter  $\alpha_2(t)$  (see Fig. 7), or  $t_{x2}$  [see Fig. 1(b)].

Thus the microscopic origin of  $t_{x2}$  is the change from primarily apparent free independent jump to the correlated jump process with modified jump angles. This fact is consistent with the independent ion jump relaxation time  $\tau_0$  being about the same as  $t_{x2}$  [Fig. 1(b)] because we expect the jumps are independent for  $t \ll \tau_0$  and more or less independent for  $t < \tau_0$ . For times from 20 ps to several hundred picoseconds, type-A and type-B ions show MSDs with time dependences  $t^p$  with  $p < 1$  and  $t^q$  with  $q > 1$ , respectively. The MSDs are less than the distance of the first minimum of  $g(r)$ , and even the type-B ions are still within neighboring sites in this time regime. Type-A and type-B ions show dynamics with different wave number dependences, naturally because only type-B ions contribute to the long time diffusion. As discussed previously in Sec. III B, a stretched exponential decay of the self-part of density correlation function  $F_s(k, t)$ , and a corresponding decrease of the area under the first peak of the self-part of van Hove function of Li ion are observed in this time regime. Hence both fast and slow dynamics have been observed in a stretched exponential region. The cause of the fast dynamics of type-B ions in the stretched exponential region and in the longer time region is the cooperative jump motion. This property has been deduced from the observation of a tracer ion, where we find that the angle of the next jump is affected by the other ions.

#### IV. CONCLUSION

The existence of the near constant loss (NCL) has been established from the molecular dynamics simulation results of Li metasilicate glass. The NCL, the very slow rise of the mean square displacement of the Li ions,  $\langle r^2 \rangle$ , and the very slow decay of the cage with time are shown to be synergistic properties in the time regime where the majority of the ions can be considered still confined within the slowly decaying cage. Ultimately, the cause of the initial cage decay is the thermally activated independent or free jumps of the Li ions from their original sites. At sufficiently low temperature and short times, there are few such free jumps but nevertheless the probability increases slowly with time. Thus the cage

decays very slowly as long as time is much shorter than the independent free jump relaxation time  $\tau_0(T)$ . This description is supported by the time dependence of the self-part of the van Hove function of the Li ion,  $G_s(r, t)$ . In fact we find in the short time regime  $t < t_{x1}$  from  $4\pi r^2 G_s(r, t)$  that the free jumps to neighboring sites are few and increase very slowly with time.

In the next or second time regime  $t_{x1} < t < t_{x2}$ , the change of  $4\pi r^2 G_s(r, t)$  with time is more rapid, indicating a more rapid decay of the cage. Concurrently, an increasingly more rapid increase of  $\langle r^2 \rangle$  is found in this time regime, but its time dependence is not a power law until after  $t_{x2}$ . In the third time regime  $t_{x2} < t < \tau$ ,  $\langle r^2 \rangle$  has the time dependence of a power law  $t^{1-n}$  with a fractional power. Here  $\tau$  is approximately the time after which  $\langle r^2 \rangle$  is proportional to  $t$ . In this third time regime, a second peak at a distance between  $\text{Li}^+$  ion sites develops in  $4\pi r^2 G_s(r, t)$  and grows with time, indicating that significant number of Li ions have jumped out of their cages to neighboring sites to participate in cooperative motion to longer distances. The self-part of the  $\text{Li}^+$  ion density correlation function  $F_s(k, t)$  in the same time regime is a stretched exponential function of time, which also is the signature of cooperative or collective dynamics. The stretch exponent of  $F_s(k, t)$  for  $k = 2\pi/10 \text{ \AA}^{-1}$  is not too different from the exponent  $(1-n)$ , appearing in the time dependence of  $\langle r^2 \rangle \propto t^{1-n}$ . We use the normalized area of the first and second peaks of  $4\pi r^2 G_s(r, t)$  to gauge the progress of the cage decay, and find that their time dependences are indicators of the change in time dependence of  $\langle r^2 \rangle$  in the three time regimes.

The real cause of the synergy between the NCL, and the very slow rise of  $\langle r^2 \rangle$  and cage decay, as a function of  $\ln t$ , is ultimately the few but nevertheless very slowly increasing number of independent free jumps of the Li ions in the time regime  $t \ll \tau_0$ . The coupling model has a prediction [Eq. (5)] that enables the independent or free jump relaxation time  $\tau_0(T)$  to be calculated from the experimental quantities  $\tau(T)$ ,  $(1-n)$ , and  $t_c$ . The value of  $t_c \approx 1$  to 2 ps is taken from previous determination of the quantity in oxide glasses. From the calculated  $\tau_0(T)$  and the correlation function  $\exp(-t/\tau_0)$  of the free jumps or its complement  $[1 - \exp(-t/\tau_0)]$ , we can see (Fig. 5) that in the early time regime 1,  $t < t_{x1} \ll \tau_0$ , the fraction of ions that have made free jumps out of the potential wells is small and increases very slowly with time. Correspondingly, the cage decay is very slow and the NCL is observed. We caution here that the cage correlation function is not given by  $\exp(-t/\tau_0)$ , even when restricted to the regime  $t < \tau_0$ . The latter gives merely an indication of the fraction of ions that have not made independent jump out of the original sites. Neither is  $A_1(t)$ , although it may have a closer relation to the cage decay function. When past time regime 1, the fraction becomes more significant, the cage decay is not very slow and the NCL, approximately described by  $\langle r^2 \rangle \propto t^\alpha$  with  $\alpha \approx 0.1$  in this work, no longer persists. It is found that  $\tau_0(T)$  is close to  $t_{x2}$ . The proximity of these two quantities means that significant fraction of Li ions have a high probability of executing their free jumps at times greater than  $t_{x2}$ , but henceforth

their motion is controlled by the heterogeneous cooperative or collective dynamics, leading eventually to long-range diffusion. The proximity further explains the onset at  $t_{x2}$  of the self-part of the Li ion density correlation function to assume the time dependence of the Kohlrausch stretched exponential function, which is the hallmark of cooperative dynamic processes in general. Recently, Heuer and co-workers [60] also have performed molecular dynamics simulation on lithium metasilicate using similar potentials. In many ways their results are similar to ours.

Although the present work is focused on the molecular dynamics simulation results of Li metasilicate, fittingly we have also brought into discussion the experimental data of colloidal supercooled liquids. The similarity in the dynamics of the two systems is remarkable. In colloidal supercooled liquids with higher volume fractions and in an extensive short time regime, the mean square displacement of the colloidal particles increases very slowly with the logarithm of time (approximately described here by  $\langle r^2 \rangle \propto t^{0.08}$ ). The crossover times  $t_{x1}$  and  $t_{x2}$ , with the same physical meanings as for the Li metasilicate, are also found in the colloidal systems. They also delineate the dynamics into several time regimes. In the colloidal systems, Weeks and Weitz obtained from a experiment that a cage decay correlation function and its time dependence is similar to that of the development of the area under the first and the second peaks of the self-part of the  $\text{Li}^+$  ion van Hove function. In particular, both systems show very slow cage decay in regime  $t < t_{x1}$ , slow decay in regime  $t_{x1} < t < t_{x2}$ , and faster decay in regime  $t > t_{x2}$ . In both systems the non-Gaussian parameter  $\alpha_2(t)$  is a broad peak with maximum at approximately  $t_{x2}$ . The dynamics is heterogeneous in both systems as demonstrated by the presence of fast and slow moving colloidal particles or  $\text{Li}^+$  ions. The distinction between fast and slow moving particles becomes increasingly clear at times after  $t_{x2}$ . The striking similarities of the two systems may or may not be due to the fact that the colloidal systems studied by Weeks and Weitz are slightly charged [61]. In spite of the similarities, the ionic glass and the supercooled colloidal liquid have differences. One difference is the presence of the much less immobile matrix atoms besides the mobile ions in the ionic glass. We have not discussed the molecular dynamics simulation results of Lennard-Jones liquid in much detail. Nevertheless, for some of the properties discussed, Lennard-Jones supercooled liquid behaves like the Li metasilicate glass and the colloidal supercooled liquid. It is likely all three systems share the same basic physics governing relaxation and diffusion of interacting particles. Therefore a theory proposed to explain the dynamics in any one of these systems is viable only if it is applicable to the other two as well.

## ACKNOWLEDGMENTS

A part of the calculations in this work was performed with an SX-3/34R and SX-5 computer at the Research Center for Computational Science. The CPU time made available is gratefully acknowledged. The work performed at the Naval Research Laboratory was supported by the Office of Naval Research.

- [1] C. T. Moynihan, *J. Non-Cryst. Solids* **172-174**, 1395 (1994); **203**, 359 (1996); *Solid State Ionics* **105**, 75 (1998).
- [2] C. T. Moynihan and L. P. Boesch, *J. Non-Cryst. Solids* **17**, 44 (1975).
- [3] F. S. Howell, R. A. Bose, P. B. Macedo, and C. T. Moynihan, *J. Phys. Chem.* **78**, 639 (1974).
- [4] C. A. Angell, *Chem. Rev.* **90**, 523 (1990).
- [5] K. L. Ngai and C. T. Moynihan, *Bull Mater. Res. Soc.* **23**, 51 (1998).
- [6] J. Wong and C. A. Angell, *Glass Structure by Spectroscopy* (Dekker, New York, 1976).
- [7] A. K. Jonscher, *Dielectric Relaxation in Solids* (Chelsea Dielectric, London, 1983).
- [8] K. Funke, *Prog. Solid State Chem.* **22**, 111 (1993).
- [9] C. Cramer, K. Funke, and T. Saatkamp, *Philos. Mag. A* **71**, 701 (1995); K. L. Ngai, C. Cramer, T. Saatkamp, and K. Funke, in *Non-Equilibrium Phenomena in Supercooled Fluids, Glasses and Amorphous Materials*, edited by M. Giordano, D. Leporini, and M. P. Tosi (World Scientific, Singapore, 1996), p. 3.
- [10] C. Cramer, K. Funke, M. Buscher, and A. Happe, *Philos. Mag. B* **71**, 713 (1995).
- [11] R. Richert and H. Wagner, *Solid State Ionics* **105**, 167 (1998).
- [12] K. Funke, B. Heimann, M. Vering, and D. Wilmer, *J. Electrochem. Soc.* **148**, A395 (2001).
- [13] R. Kohlrausch, *Ann. Phys. (Leipzig)* **72**, 393 (1847).
- [14] A. Burns, G. D. Chryssikos, E. Tombari, R. H. Cole, and W. M. Risen, *Phys. Chem. Glasses* **30**, 264 (1989).
- [15] W. K. Lee, J. F. Liu, and A. S. Nowick, *Phys. Rev. Lett.* **67**, 1559 (1991); A. S. Nowick, A. V. Vaysleb, and W. Liu, *Solid State Ionics* **105**, 121 (1998); A. S. Nowick, B. S. Lim, and A. V. Vaysleb, *J. Non-Cryst. Solids* **172-174**, 1243 (1994).
- [16] X. Lu and H. Jain, *J. Phys. Chem. Solids* **55**, 1433 (1994).
- [17] C. H. Hsieh and H. Jain, *J. Non-Cryst. Solids* **203**, 293 (1996).
- [18] J. Dieckhoeffler, O. Kanert, R. Kuchler, A. Volmari, and H. Jain, *Phys. Rev. B* **55**, 14 836 (1997).
- [19] K. L. Ngai, *J. Chem. Phys.* **110**, 10 576 (1999).
- [20] A. K. Rizos, J. Alifragis, K. L. Ngai, and P. Heitjans, *J. Chem. Phys.* **114**, 931 (2001).
- [21] C. Leon, A. Rivera, A. Varez, J. Sanz, J. Santamaria, and K. L. Ngai, *Phys. Rev. Lett.* **86**, 1279 (2001).
- [22] K. L. Ngai and C. Leon, *Phys. Rev. B* (to be published).
- [23] P. Lunkenheimer, A. Pimenov, and A. Loidl, *Phys. Rev. Lett.* **78**, 2995 (1997).
- [24] P. Lunkenheimer, *Dielectric Spectroscopy of Glassy Dynamics* (Shaker, Aachen, 1999).
- [25] K. L. Ngai, *Comments Solid State Phys.* **9**, 121 (1979).
- [26] K. Y. Tsang and K. L. Ngai, *Phys. Rev. E* **54**, R3067 (1996).
- [27] K. Y. Tsang and K. L. Ngai, *Phys. Rev. E* **56**, R17 (1997).
- [28] R. W. Rendell, *Phys. Rev. E* **48**, R17 (1993); *J. Appl. Phys.* **75**, 7626 (1994).
- [29] K. L. Ngai and K. Y. Tsang, *Phys. Rev. E* **60**, 4511 (1999).
- [30] K. L. Ngai, R. W. Rendell, and H. Jain, *Phys. Rev. B* **30**, 2133 (1984).
- [31] G. N. Greaves and K. L. Ngai, *Phys. Rev. B* **52**, 6358 (1995).
- [32] K. L. Ngai, G. N. Greaves, and C. T. Moynihan, *Phys. Rev. Lett.* **80**, 1018 (1998).
- [33] K. L. Ngai, *Philos. Mag. A* **77**, 187 (1998).
- [34] K. L. Ngai and A. K. Rizos, *Phys. Rev. Lett.* **76**, 1296 (1996).
- [35] C. Cramer, K. Funke, M. Buscher, and A. Happe, *Philos. Mag. B* **71**, 713 (1995); K. L. Ngai, C. Cramer, T. Saatkamp, and K. Funke, in *Non-Equilibrium Phenomena in Supercooled Fluids, Glasses and Amorphous Materials* (Ref. [9]).
- [36] C. Cramer and M. Buscher, *Solid State Ionics* **105**, 109 (1998).
- [37] K. L. Ngai, *J. Non-Cryst. Solids* **248**, 194 (1999).
- [38] S. Chandrasekhar, *Rev. Mod. Phys.* **15**, 1 (1943).
- [39] C. Huang and A. N. Cormack, *J. Chem. Phys.* **95**, 3634 (1991).
- [40] W. Smith, N. Greaves, and M. J. Gillan, *J. Chem. Phys.* **103**, 3091 (1995).
- [41] S. Balasubramian and K. J. Rao, *J. Non-Cryst. Solids* **181**, 157 (1995).
- [42] J. Habasaki, I. Okada, and Y. Hiwatari, *J. Non-Cryst. Solids* **183**, 12 (1995).
- [43] J. Habasaki, I. Okada, and Y. Hiwatari, *Phys. Rev. E* **52**, 2681 (1995).
- [44] J. Habasaki, I. Okada, and Y. Hiwatari, *Prog. Theor. Phys. Suppl.* **126**, 399 (1997).
- [45] J. Habasaki, Y. Hiwatari, and I. Okada, *Mater. Res. Soc. Symp. Proc.* **455**, 91 (1997).
- [46] J. Habasaki, I. Okada, and Y. Hiwatari, *Phys. Rev. B* **55**, 6309 (1997).
- [47] J. Habasaki, I. Okada, and Y. Hiwatari, *J. Phys. Soc. Jpn.* **67**, 2012 (1998).
- [48] J. Habasaki and Y. Hiwatari, *Phys. Rev. E* **58**, 5111 (1998).
- [49] J. Habasaki and Y. Hiwatari, *Phys. Rev. E* **59**, 6962 (1999).
- [50] E. R. Weeks and D. A. Weitz, e-print cond-mat/0107279; *Phys. Rev. Lett.* (to be published).
- [51] The Haven ratio has been taken to be approximately independent of frequency, since it varies usually by only as much as a factor of 2 for several decades in frequency, and in fact it has a value of 1 at high frequencies.
- [52] Y. Ida, *Phys. Earth Planet. Inter.* **13**, 97 (1976).
- [53] J. Habasaki and I. Okada, *Mol. Simul.* **9**, 319 (1992).
- [54] K. L. Ngai, *Phys. Rev. B* **48**, 13 481 (1993).
- [55] K. L. Ngai and C. Leon (unpublished).
- [56] K. L. Ngai, *J. Phys. (Paris), Colloq.* **2**, 61 (1992); K. L. Ngai and O. Kanert, *Solid State Ionics* **53-55**, 936 (1992).
- [57] A. Rahman, *Phys. Rev.* **136**, A405 (1964).
- [58] E. R. Weeks, J. C. Crocker, A. Levitt, A. Schofield, and D. A. Weitz, *Science* **287**, 627 (2000).
- [59] W. Kob, C. Donati, S. J. Plimton, P. H. Poole, and S. C. Glotzer, *Phys. Rev. Lett.* **79**, 2827 (1997).
- [60] A. Heuer, M. Kunow, M. Vogel, and R. D. Banhatti, e-print cond-mat/0205547; *Phys. Chem. Chem. Phys.* (to be published).
- [61] E. R. Weeks (private communication).